The Effect of Slurry Type on Drilled Shaft Cover Quality

Sarah Mobley, MSCE, P.E.[1] and Kelly Costello, MSCE, E.I.[2]

ABSTRACT

Until recently, concrete flow in tremie-placed drilled shafts has been mischaracterized as rising uniformly with laitance formation occurring at the top of the shaft. In actuality, concrete first fills a portion of the reinforcement cage prior to flowing radially to the cover region. Depending on slurry type, the radial flow can produce laitance-filled creases/channels that project the reinforcing cage configuration to the side of shaft surface. The flow pattern (and creases) can affect filter cake thickness, cover quality and propensity for corrosion. This paper examines 24 tremie-placed laboratory drilled shaft specimens, constructed using bentonite, polymer or natural slurry to identify correlations between slurry type and laitance channel formation. The extent of the laitance channel effects was quantified with surface texture, corrosion potential, and strength distribution methods. A direct correlation between the use of bentonite slurry and laitance channel formation was identified which showed a high propensity for corrosion and lower strengths. Shafts cast using polymer behaved the same as the shafts cast using water, neither of which showed a heightened propensity for corrosion or reduction in strength.

INTRODUCTION

When considering the significance of the concrete quality in a drilled shaft, it becomes apparent the cover region is most important. This cover region contributes far more to the bending moment of inertia than the core concrete within the cage, forms the mechanical/structural bond to the surrounding bearing strata, and provides a barrier from external chemical agents that promote corrosion (e.g. chlorides or sulfates). Until recently, this portion of drilled shaft concrete could not be adequately tested via non-destructive integrity methods and went largely unassessed. The implication being that there may be shafts in service with flaws in the cover. With regards to the focus of this study, the ability or inability of drilled shaft concrete to freely flow into the annular cover region and maintain the desired concrete properties can have the most dire effects on durability / longevity of the overall structural integrity.

The goal of this study was to create and implement methods that describe the electrochemical, physical and strength characteristics of 24 test shaft specimens tremie-placed in varied slurry conditions. This investigation was subdivided into three methods of assessing the as-built quality of the shafts: (1) side-of-shaft surface texture / void volume determination, (2) corrosion protection, and (3) coring with dynamic strength profiling and compressive strength testing.

[1] Doctoral Student, Department of Civil and Environmental Engineering, University of South Florida, Tampa, FL; sarahmobley@mail.usf.edu

[2] Doctoral Candidate, Department of Civil and Environmental Engineering, University of South Florida, Tampa, FL; kcostell@mail.usf.edu

BACKGROUND

Despite advances in specifications and non-destructive testing, the true quality of blindly built drilled shafts remains unknown The three factors that determine drilled shaft quality are reinforcement cage dimensions, slurry quality and concrete properties where concrete flow properties are the probable cause for all anomalies both known and unknown.

Concrete rising in slurry filled excavations forms a layer / interface between concrete and the slurry or water that is being displaced. This zone of diffusion and mixing is commonly referred to as laitance. However, past studies have shown that concrete does not simply displace slurry like oil over water but rather builds-up a certain amount of head inside the cage prior to pushing through the reinforcing cage in a radial flow pattern. (Deese and Mullins, 2005; Brown, 2004) Deese and Mullins showed the height of concrete buildup inside the cage was proportional to the square of upward velocity and inversely proportional to the clear rebar spacing (Figure 1). As the concrete flows through the reinforcement cage it is cleaved by the vertical and horizontal rebar and then rejoins on the outside of the cage. This provides an inherit opportunity for laterally forming laitance interfaces to become trapped creating a crease (Figure 2). These creases often extend to the surface and reflect the reinforcement cage layout (Figure 3); this phenomenon is termed *mattressing* by the Deep Foundations Institute (Beckhaus, 2016).

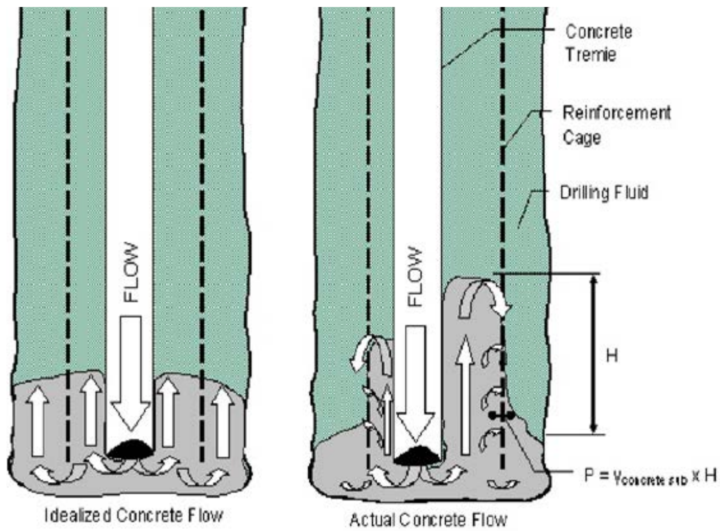

Figure 1: Actual vs idealized flow (Deese and Mullins, 2005).

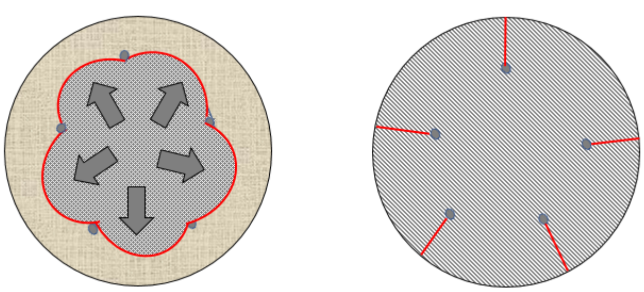

Figure 2: Laitance crease formation (red lines)

Figure 3: Mattressing in a drilled shaft

The potential negative impacts of flow-induced anomalies and laitance crease formation are threefold: (1) laitance channels can create direct pathways for the transmission of environmental chlorides to reach the reinforcing steel network, negating the protective qualities of the concrete cover and increasing the opportunity for corrosion, (2) the presence of trapped laitance can compromise the strength of the cover region and reduce structural capacity such as cracking and ultimate bending strength, and (3) the presence of trapped laitance and slurry along the shaft side walls has been attributed to filter cake formation even in low permeability soils. While filter cake formation is not the focus of this study, trapped laitance or slurry can be quantified by the surface texture for later consideration.

RESEARCH SIGNIFICANCE

The findings of this study as well as the ongoing work, promise to increase awareness of the effects of slurry type on drilled shaft durability and better explain side shear degradation in the presence of bentonite slurry with applications extending even into low permeability soils not prone to filtering.

APPROACH

Twenty four - 42in diameter drilled shaft specimens were cast over a 2 year period from 2013 to 2015. Concrete was tremie placed in water, polymer or bentonite slurry having a wide range of Marsh funnel viscosities. Despite being cast in steel forms, bentonite specimens were recognizably distressed at the time of form removal with bentonite caking trapped in visible creases (Mullins and Winters, 2014; Bowen, 2014). After only 4 years of outdoor exposure, the surface of the bentonite specimens notably degraded. Identifying the cause of the creases and degradation remained a primary motivation for this study. Testing procedures were developed to quantify the surface texture, state of corrosion, and concrete strength.

Surface Texture

Much of this study revolved around identifying physical surface features that may indicate concrete flow problems and potential adverse effects on the longevity of the structure. To this end, the surface condition of the shafts was an obvious variable for consideration. Two methods were used: physical surface void volume measurements and digital 3-D scanning.

Physical Measurements: The surface roughness was assessed by measuring the volume of putty required to fill the surface voids (Costello et al., 2017). The void volume was measured at two representative areas by recording the weight of the putty, with known density, required to make the surface smooth. This volume was then extrapolated to approximate the void volume for the entire shaft surface. This assumed the original outer surface of the shaft had not undergone severe radial reduction and that the putty would produce a smooth surface representative of an undamaged shaft surface (Figure 4).

Figure 4: Putty void volume test

Digital Scanning: One side of each shaft was also scanned using an Artec Eva 3D scanner which produced a digital rendering of the shaft surface down to 10 micron accuracy (Figure 5). The three dimensional surface was analyzed using the corridor modeling tools in AutoCAD Civil3D to determine the volume required to restore a smooth surface. This required robust computational capabilities to handle the 3-5 million data points; only three of the shafts are presented herein.

Figure 5: Scanning specimen (left), shaft photo (center), digital rendering (right).

Corrosion

Surface potential measurements are a strong indicator of active corrosion within a reinforced concrete structure. This test is performed by measuring the relative voltage potential between the reinforcing steel and a copper-copper sulfate electrode in wetted contact with the concrete surface several inches away from the reinforcing steel (ASTM, 2009).When the measured potential is more negative than -350mV there is a high probability of corrosion.

Figure 6: Surface potential testing

The surface potential of each shaft specimen was mapped evenly over the surface using a prescribed grid layout. A template was made out of sheet of 21-inch by 27-inch rubberized plastic. A sharpened 2-inch diameter pipe was used to punch holes through the plastic in rows with a 3-inch CTC spacing in both directions. This resulted in 80 measurement locations for each shaft. The shafts were wetted and surface potential testing was then conducted per ASTM C876-09: *Standard Test Method for Corrosion Potentials of Uncoated Reinforcing Steel in Concrete*, using a copper-copper sulfate reference electrode and a standard multi-meter (Figure 6).

Strength Variation

A fully instrumented coring machine, hereafter referred to as a concrete penetrometer, was developed to record variations in concrete strength while collecting a core sample (Figure 7). The penetrometer computes strength (f'_c) by eliminating variables in two torque equations: mechanical and electrical. Measured parameters include: crowd, rpm, torque, displacement, cutting fluid flow rate and fluid pressure. Complete details of the instrumentation and data analysis can be found elsewhere (Costello et al., 2017).

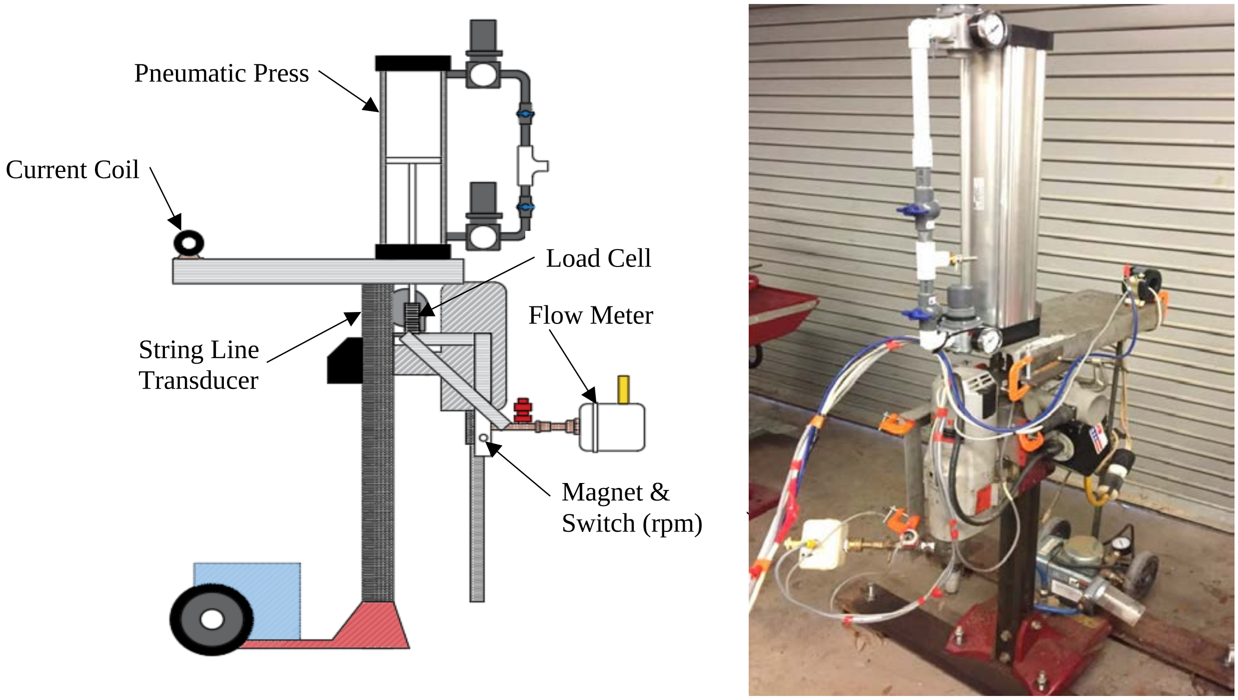

Figure 7: Concrete Penetrometer

RESULTS

The test results reference the 24 shaft specimens by the Shaft ID number, the slurry type (W, water; P, polymer; or B, bentonite), the Marsh funnel viscosity. Additionally, in two cases self-consolidated concrete is denoted as SCC. All other shafts were cast with Class IV Drilled Shaft mix per FDOT specification (FDOT, 2016 standard specifications). For example, 11-P65 was Shaft 11, cast in polymer, viscosity was 65 sec/qt, and Class IV concrete is implied.

Physical Void Volume: Void volume was computed for two test areas on each shaft, the results were then averaged and extrapolated over the entire shaft surface (Table 1). The values range from 38 to 592in^3. Note 24-B40, SCC was not tested due to severe surface degradation.

Table 1: Physical Void Volume Data

Shaft Name	Total Void Volume (in^3)	Shaft Name	Total Void Volume (in^3)	Shaft Name	Total Void Volume (in^3)
6-W	41.9	17-P85	38.2	1-B44	592.3
18-W	47.4	20-P130	32.7	9-B50	260.2
22-W	29.6	7-B30	487.2	4-B55	313.2
23-W, SCC	48.1	13-B30	167	15-B56	263.2
19-P60	43.3	14-B30	299.5	5-B90	253.8
11-P65	71.4	3-B40	203.4	10-B90	540.1
12-P66	59.4	8-B40	215.2	2-B105	491.6
16-P85	72.6	21-B40	577.6	24-B40, SCC	-

Digital Void Volume: The digital void volume method superimposes a perfect shaft surface over the digitally recorded 3-D shaft surface. It uses the highest measured points within the selected area to determine the ideal curved shaft surface. The volume required to fill the digitally measured surface up to the ideal surface was then recorded. Digital surface void volume determination resulted in higher quantities than the physical method (Table 2). This could be due to the reference ideal surface used and the physical void volume ideal surface is created without a template and as such is left to the judgement of the technician performing the test. The percent difference shown below illustrates the conservative nature of the physical method.

Table 2: Digital surface void volume data

Shaft Name	6-W	11-P60(65)	9-B50
Physical Void Volume Per Total Surface Area (in^3)	42	71	260
Digital Void Volume Per Total Surface Area (in^3)	53.55	80.84	302.12
Percent Increase From Physical Volume	22%	12%	14%

Corrosion Potential: The copper-copper sulfate testing for each shaft included 80 data points. The 50th percentile (E_{50}) potential value was determined for each shaft. These values ranged from -508mV to -155mV (Table 3). Thirty five percent of the test shafts had E_{50} potentials below -350mV and all of those shafts were constructed using bentonite slurry (Table 3). Surface potential contours for a water, polymer and bentonite shaft are shown in Figure 8. Grey shades from light (good) to dark (bad) show at a glance the state of the bentonite shaft relative to the others.

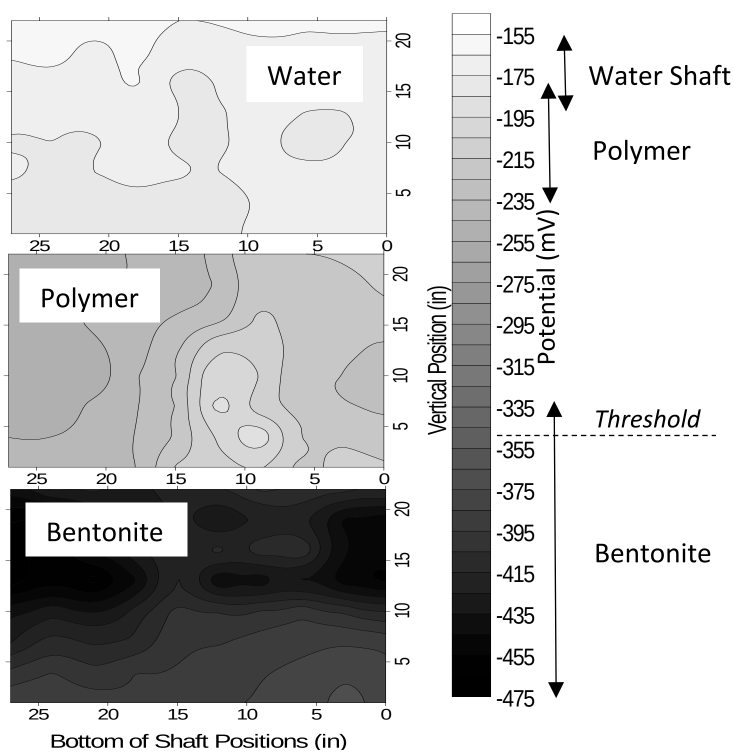

Figure 8: Corrosion potential contours

Table 3: E_{50} potential

Shaft Name	E_{50} (mV)
6-W	-155
18-W	-293
22-W	-250
23-W, SCC	-258
19-P60	-243
11-P65	-285
12-P66	-190
16-P85	-279
17-P85	-300
20-P130	-242
7-B30	**-372**
13-B30	-289
14-B30	-282
3-B40	**-373**
8-B40	-225
24-B40-SCC	**-425**
21-B40	**-508**
1-B44	-317
9-B50	**-383**
4-B55	-443
15-B56	-335
5-B90	**-447**
2-B105	**-449**

Strength Profiles: Concrete penetrometer testing was performed in four locations on each of three subject shafts, two in the core and two in the cover. Figures 9,10 and 11 show the average cover and core strengths for a water, polymer and bentonite shaft, respectively.

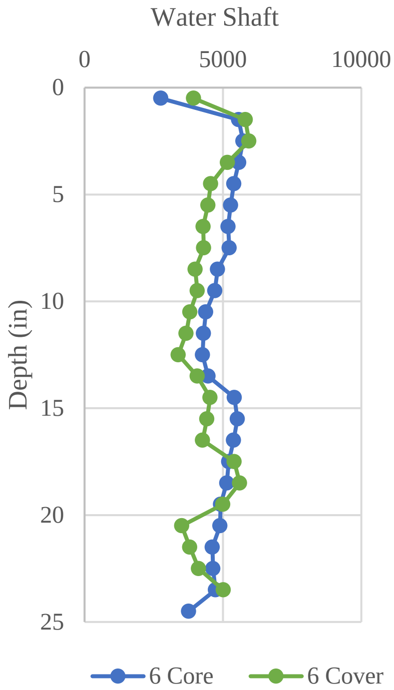

Figure 9: Shaft 6-W

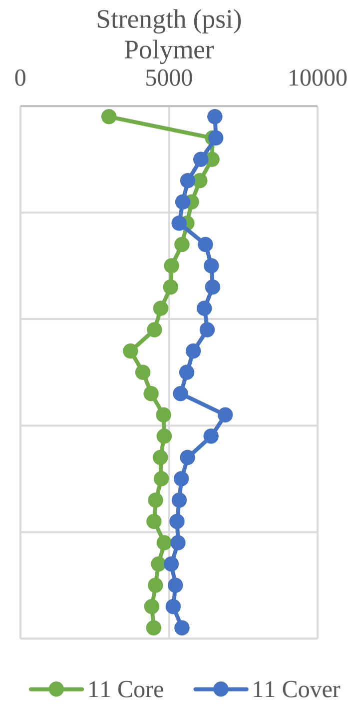

Figure 10: Shaft 11-P65

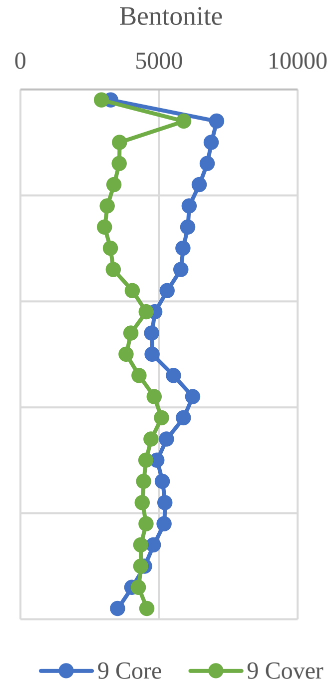

Figure 11: Shaft 9-B50

Water shaft 6-W (Figure 9) was cast as a control and demonstrates a generally uniform profile between samples. The close grouping of the data shows consistency in the concrete strength profile which was expected in the control samples. Polymer shaft 11-P65 (Figure 10) showed similar consistency.

Figure 11 shows the average strength profiles for specimen 9-B50 ranged from 3200 to 7000psi. While more samples need to be cored to corroborate the noted trends, the conclusion currently drawn is that the bentonite shafts did not yield uniform strength profiles and that the concrete strength is reduced in the cover region.

DISCUSSION

The average surficial void volume for all water, polymer and bentonite shafts was 42, 53, and 359in^3, respectively from putty tests. The digitally predicted values for the three completed specimens to date were 54, 81, and 302in^3, again respectively. Even without chemical analyses of the cover concrete (pending), there is reason to investigate the mechanism that caused degradation. As all specimens were cast with steel removable forms, filtration into the surrounding soil could not occur, yet bentonite slurry was found caked along the sides of all bentonite shafts. The radial flow of concrete into the cover region is thought to have trapped the “filter cake” like material.

The average E_{50} potential values for all water, polymer and bentonite specimens were -239, -257, and -373mV, respectively. This confirms corrosion protection for water and polymer specimens but highlights the original concerns about the cover quality of bentonite shafts. Seventy percent of all bentonite specimens exhibited E_{50} surface potentials below the -350mV corrosion threshold and 92% of bentonite samples exhibited localized critical potential values somewhere in the measured data field. The bentonite shafts exhibit a general trend between E_{50} potential and surface void volume (Figure 12) wherein the potential becomes more negative as the void volume increases. No specimens were subjected to chlorides which can exacerbate low surface potentials, yet the steel in these shafts was actively corroding. Further, computations for life span expectancy from corrosion protection assume homogeneous cover material which is invalid as soon as cracking or any other chloride pathway is provided.

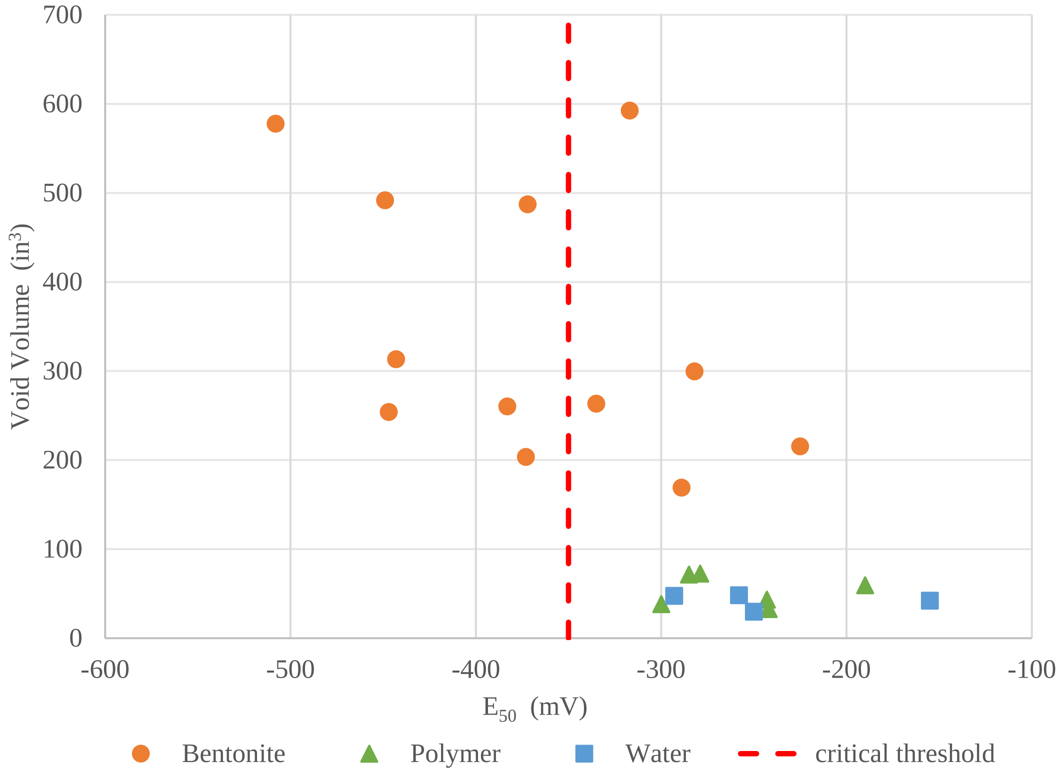

Figure 12: Void Volume vs. E_{50} Potential for all shafts

When considering the effects of viscosity on cover quality, Figure 13 shows that the critical corrosion potential was observed for all values of viscosity for the shafts constructed in bentonite slurry. This suggests that the mere presence of bentonite slurry as the concrete flows through and around the rebar is enough to compromise durability.

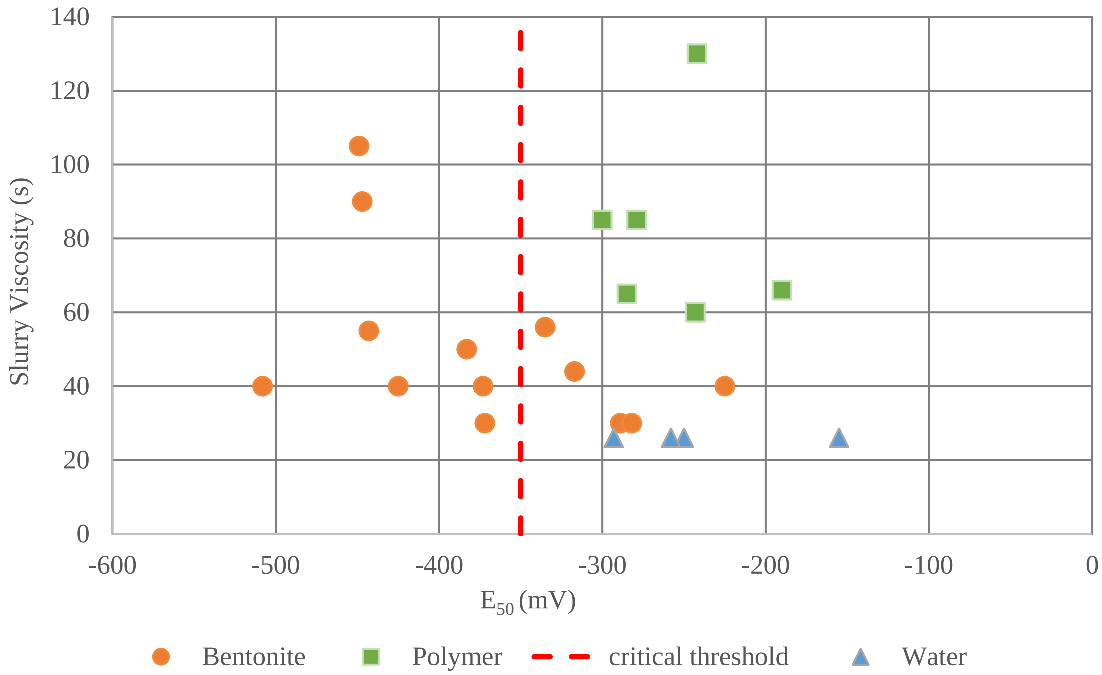

Figure 13: Slurry Viscosity vs. E_{50} Potential for all shafts

The average concrete strength in the cover of the water, polymer and bentonite shafts were 4465, 5586 and 4116 psi, respectively. The modest variation in strength indicated that the concrete quality between laitance creases was relatively unaffected and the coring only encountered trapped laitance intermittently. These thin lenses did not significantly affect the average strength. However, where 100% recovery was observed for all shafts, cores from bentonite shafts were a collection of short lengths where breaks corresponded to the exact horizontal crease locations (Figure 14). All water and polymer cores were full length and unbroken. When considering cracking moment computations a mattressed shaft is essentially already cracked resulting in a cracking moment of zero.

Figure 14: Cores extracted from Shaft 9-B50 (bottom two specimens extracted from the cover region)

CONCLUSION

In an attempt to identify the reason for bentonite shafts consistently forming creases in large scale laboratory specimens, a test program was undertaken to screen twenty four 42in diameter specimens for shaft side surface roughness, corrosion potential and strength variation. Given the extreme importance of the cover concrete, any unknown conditions that are caused by a given construction material should be fully vetted. Results of the testing showed that specimens cast in water or polymer slurry were without significant flaws. Specimens cast in bentonite slurry, regardless of viscosity, all showed severe surface degradation. Where the occurrence of mattressing was originally thought to be an abnormal exception, in bentonite construction it actually may be the norm.

REFERENCES

ASTM C876-09: *Standard Test Method for Corrosion Potentials of Uncoated Reinforcing Steel in Concrete* Annual Book of ASTM Standards, ASTM International, West Conshohocken, Pennsylvania.

Beckhaus, K. (2016). *EFFC/DFI Best Practice Guide to Tremie Concrete for Deep Foundations* (1st ed.). Hawthorne, NJ: Deep Foundations Institute.

Brown, D. (2004). "Recipe for Success with Drilled Shaft Concrete," *Foundation Drilling Magazine*, 16-24.

Brown, D. A., Turner, J. P., & Castelli, R. J. (2010). *Drilled shafts: construction procedures and LRFD design methods*. McLean, VA: U.S. Dept. of Transportation, Federal Highway Administration.

Costello, K., Mobley, S. and Mullins, G. (2017) "Evaluation of Self Consolidating Concrete and Class IV Concrete Flow in Drilled Shafts- Part 1", FDOT Project No. BDKV25-TW0977-25, Chapter 3, p91-287

Deese, G. and Mullins, G. (2005). " Factors Affecting Concrete Flow in Drilled Shaft Construction," ADSC GEO3, GEO Construction Quality Assurance / Quality Control Conference Proceedings, Bruce, D.A. and Cadden, A. W. (eds) pp. 144-155, November

Mullins, G. and Winters, D. (2014) Defining the Upper Viscosity Limit for Mineral Slurries used in Drilled Shaft Construction, FDOT Project No. BDK84-977-24, Final Report, 264 pp.